

## Direct Detection of Formate Ligation in Cytochrome *c* Oxidase by ATR-FTIR Spectroscopy

Masayo Iwaki and Peter R. Rich\*

Contribution from the The Glynn laboratory of Bioenergetics, Department of Biology, University College London, Gower Street, London WC1E 6BT, U.K.

Received October 30, 2003; E-mail: prr@ucl.ac.uk

**Abstract:** The IR signature of binding of formate to the heme  $a_3$ -Cu<sub>B</sub> binuclear site of bovine cytochrome *c* oxidase has been obtained by perfusion ATR-FTIR spectroscopy. The data show unequivocally that formate binds in its anionic form despite its binding being electroneutral overall. The bound formate can be distinguished from free ligand by the binding-induced sharpening and downshifting of vibrational bands. Formate ligation also causes shifts of vibrational modes of heme  $a_3$  and its substituents and perturbation of histidine residues. The association of the accompanying protonation change with a carboxylate or tyrosine can be ruled out and may involve a histidine metal ligand or, more likely, a simple displacement into the bulk phase of a hydroxide ligand to heme  $a_3$  or Cu<sub>B</sub>, a reaction which would account for stoichiometric proton uptake and maintenance of net charge within the binuclear center domain.

### Introduction

Cytochrome *c* oxidase (CcO) is the terminal enzyme of the mitochondrial and many bacterial respiratory chains. It catalyzes the four-electron reduction of dioxygen to water and is coupled to generation of a protonmotive force that can drive ATP synthesis. Atomic structures have been determined for CcO from bovine heart,<sup>1</sup> *Paracoccus denitrificans*,<sup>2</sup> *Thermus thermophilus*,<sup>3</sup> and *Rhodobacter sphaeroides*.<sup>4</sup> The catalytic site that binds dioxygen is formed from heme  $a_3$  and Cu<sub>B</sub>. In its oxidized state, this binuclear center has a propensity to change ligation properties to form a variety of relatively unreactive states. However, the catalytically relevant state is the “fast” form that can be identified by rapid reducibility of both hemes, a Soret absorption maximum at 424 nm, and rapid reactivity with ligands such as carbon monoxide, cyanide, azide, and formate.<sup>5–7</sup> It has been proposed that one or both metals are ligated by hydroxide ions in this “fast” form of oxidized CcO,<sup>8,9</sup> and direct evidence for hydroxide ligation of heme  $a_3$  has been provided by Raman<sup>10</sup> and EPR<sup>11</sup> studies. Formate ligation has been

examined by visible, EPR, and magnetic circular dichroism spectroscopies. The results show that formate binds only to the oxidized binuclear center, causing the heme  $a_3$  to become more high spin<sup>12</sup> and leading to an unusual EPR signal at  $g = 12$ <sup>7,13,14</sup> whose features can be simulated only with the assumption of very weak spin coupling between heme  $a_3$  and Cu<sub>B</sub><sup>15</sup> and are suggestive of formate acting as a bridging ligand between the metal centers. A similar high  $g$  value feature is found in the unreactive “resting” form of CcO that tends to form spontaneously at low pH,<sup>6,16–18</sup> again indicative of a bridged structure of some kind. To date, however, no atomic structures are available for either formate-ligated or “resting” forms of CcO and their structures are still poorly understood. Formate binding is also known to be electrostatically neutral as anion binding ( $pK_a$  3.74) is accompanied by the loss of proton from the surrounding medium,<sup>19</sup> though again the internal protonation site involved is not known. Here we address these questions by direct observation of binding of formate to the binuclear site of bovine CcO by perfusion-induced attenuated total reflection Fourier transform infrared (ATR-FTIR) spectroscopy.

### Materials and Methods

Cytochrome oxidase was isolated from bovine heart mitochondria in the oxidized “fast” form.<sup>7</sup> After removal of excess detergent, a thin film (0.05 mg protein total) was deposited on the surface of a 3 mm

- (1) Tsukihara, T.; Aoyama, H.; Yamashita, E.; Tomizaki, T.; Yamaguchi, H.; Shinzawa-Itoh, K.; Nakashima, R.; Yaono, R.; Yoshikawa, S. *Science* **1996**, *272*, 1136–1144.
- (2) Iwata, S.; Ostermeier, C.; Ludwig, B.; Michel, H. *Nature* **1995**, *376*, 660–669.
- (3) Soulimane, T.; Buse, G.; Bourenkov, G. P.; Bartunik, H. D.; Huber, R.; Than, M. E. *EMBO J.* **2000**, *19*, 1766–1776.
- (4) Svensson-Ek, M.; Abramson, J.; Larsson, G.; Törnroth, S.; Brzezinski, P.; Iwata, S. *J. Mol. Biol.* **2002**, *321*, 329–339.
- (5) Nicholls, P.; Petersen, L. C.; Miller, M.; Hansen, F. B. *Biochim. Biophys. Acta* **1976**, *449*, 188–196.
- (6) Moody, A. J. *Biochim. Biophys. Acta* **1996**, *1276*, 6–20.
- (7) Moody, A. J.; Cooper, C. E.; Rich, P. R. *Biochim. Biophys. Acta* **1991**, *1059*, 189–207.
- (8) Babcock, G. T.; Wikström, M. *Nature* **1992**, *356*, 301–309.
- (9) Mitchell, R.; Mitchell, P.; Rich, P. R. *Biochim. Biophys. Acta* **1992**, *1101*, 188–191.
- (10) Ogura, T.; Hirota, S.; Proshlyakov, D. A.; Shinzawa-Itoh, K.; Yoshikawa, S.; Kitagawa, T. *J. Am. Chem. Soc.* **1996**, *118*, 5443–5449.
- (11) Brändén, M.; Namslauer, A.; Hansson, O.; Aasa, R.; Brzezinski, P. *Biochemistry* **2003**, *42*, 13178–13184.

- (12) Babcock, G. T.; Vickery, L. E.; Palmer, G. *J. Biol. Chem.* **1976**, *251*, 7907–7919.
- (13) Brudvig, G. W.; Stevens, T. H.; Morse, R. H.; Chan, S. I. *Biochemistry* **1981**, *20*, 3912–3921.
- (14) Schoonover, J. R.; Palmer, G. *Biochemistry* **1991**, *30*, 7541–7550.
- (15) Hunter, D. J. B.; Oganessian, V. S.; Salerno, J. C.; Butler, C. S.; Ingledew, W. J.; Thomson, A. J. *Biophys. J.* **2000**, *78*, 439–450.
- (16) Brunori, M.; Colosimo, A.; Sarti, P.; Antonini, E.; Wilson, M. T. *FEBS Lett.* **1981**, *126*, 195–198.
- (17) Baker, G. M.; Noguchi, M.; Palmer, G. *J. Biol. Chem.* **1987**, *262*, 595–604.
- (18) Palmer, G.; Baker, G. M.; Noguchi, M. *Chem. Scr.* **1988**, *28A*, 41–46.
- (19) Mitchell, R.; Rich, P. R. *Biochim. Biophys. Acta* **1994**, *1186*, 19–26.

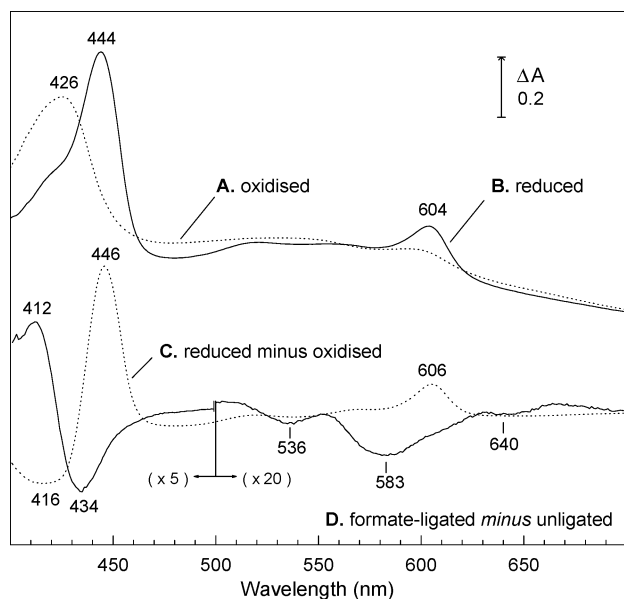


**Figure 1.** Visible absorption spectra of a film of bovine CcO on an ATR prism: (A) aerobically oxidized; (B) fully reduced on perfusion with 3 mM sodium dithionite; (C) reduced minus oxidized difference spectrum (B minus A); (D) formate-ligated minus unligated oxidized state after washing out of free formate. Spectra were measured in 0.1 M potassium phosphate and 0.2 M KCl at pH 6.5 and at room temperature.

diameter silicon ATR microprism (three bounce version, SensIR Europe) as described previously.<sup>20</sup> The hydrophobically attached protein film was rehydrated in a buffer of 0.1 M potassium phosphate and 0.2 M KCl at pH 6.5, and a chamber was then mounted over the protein film that enabled switching of perfusate buffers. Visible/near UV optical changes were monitored at the same time as IR difference spectra with a scanned beam that was passed through the sample and collected after reflection off the top of the prism surface as described previously.<sup>20</sup> Fully oxidized CcO was generated from the dithionite-reduced state by perfusion of aerobic buffer containing 1 mM potassium ferricyanide for 1 min, followed by aerobic buffer alone. This ensured that the enzyme remained in the reactive “fast” form, and subsequent perfusion with buffer containing 10 mM potassium formate for 3 min induced maximal formate binding. Once bound, free formate could be omitted from the perfusate without measurable dissociation from CcO, allowing measurement of binding-induced difference spectra without interference from free formate. To regenerate the unligated oxidized state, the enzyme was reduced by perfusion with buffer containing 3 mM sodium dithionite, causing the formate to dissociate,<sup>21</sup> after which the oxidized, unligated state was regenerated as above. FTIR spectra were recorded with a Bruker IFS 66/S spectrometer equipped with a liquid nitrogen cooled MCT-A detector and configured for ATR measurements. Typically, three to four cycles of measurement with five different samples were recorded and averaged, with each measurement being the average of 2000 interferograms. All measurements were made at room temperature with a resolution of 4 cm<sup>-1</sup>. For experiments in D<sub>2</sub>O, all media for sample preparation and manipulation were replaced by equivalent D<sub>2</sub>O media and with pD adjusted using pD = pH meter reading + 0.4.<sup>22</sup> At the start of experiments, by which time the sample had been exposed to D<sub>2</sub>O for at least 10 h, the extent of H/D exchange was estimated to be >90% by calculation according to ref 23.

## Results and Discussion

Figure 1 shows the visible absorption spectra of the CcO film under oxidizing (Figure 1A) and reducing (Figure 1B) condi-

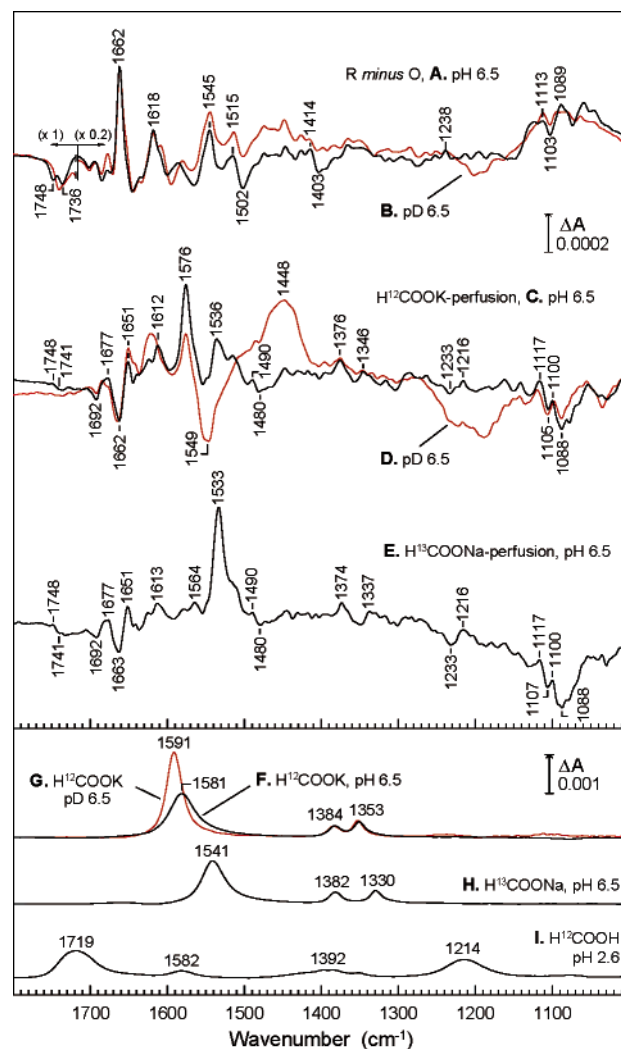


**Figure 2.** Perfusion-induced ATR-FTIR difference spectra of a film of bovine CcO on an ATR prism. IR spectra were recorded synchronously with corresponding visible difference spectra of Figure 1. Upper panel: reduced minus oxidized difference spectra in (A) H<sub>2</sub>O media at pH 6.5, (B) D<sub>2</sub>O media at pD 6.5, (C) formate-ligated minus unligated difference spectra after washing away of free formate in H<sub>2</sub>O media at pH 6.5 with <sup>12</sup>COOK, (D) D<sub>2</sub>O media at pD 6.5 with <sup>12</sup>COOK, and (E) H<sub>2</sub>O media at pH 6.5 with <sup>13</sup>COONa. Where necessary, a baseline correction was applied to eliminate the contribution of protein swelling/shrinkage. Lower panel: ATR-FTIR absolute spectra of 10 mM <sup>12</sup>COOK in H<sub>2</sub>O media at pH 6.5 (F) and in D<sub>2</sub>O media at pD 6.5 (G), 10 mM <sup>13</sup>COONa in H<sub>2</sub>O media at pH 6.5 (H), and 10 mM <sup>12</sup>COOH in distilled water at pH 2.6 (I). All spectra were measured at room temperature, and absorption due to buffer and solvent has been subtracted.

tions. These spectra, and the derived reduced minus oxidized spectrum (Figure 1C; =1B minus 1A), exhibit peaks/troughs characteristic of “fast” oxidized CcO.<sup>24</sup> The corresponding reduced minus oxidized IR difference spectrum, measured simultaneously with these visible spectra, is shown in Figure 2, traces A (H<sub>2</sub>O media) and B (D<sub>2</sub>O media). This spectrum is very similar to those reported previously at pH 8.5<sup>25</sup> and 9<sup>20</sup> and argues strongly against pH-dependent conformers of CcO in this pH range. This similarity extends to the troughs at 1748

(22) Glasoe, P. K.; Long, F. A. *J. Phys. Chem.* **1960**, *64*, 188–190.

(23) Rath, P.; DeGrip, W. J.; Rothschild, K. J. *Bioophys. J.* **1998**, *74*, 192–198.

(24) Rich, P. R.; Moody, A. J. In *Bioelectrochemistry: principles and practice*; Gräber, P., Milazzo, G., Eds.; Birkhäuser Verlag AG: Basel, 1997; pp 419–456.

(25) Rich, P. R.; Breton, J. *Biochemistry* **2002**, *41*, 967–973.

(20) Iwaki, M.; Puustinen, A.; Wikström, M.; Rich, P. R. *Biochemistry* **2003**, *42*, 8809–8817.

(21) Chang, K. T.; Palmer, G. *Biochim. Biophys. Acta* **1996**, *1277*, 237–242.

and 1736  $\text{cm}^{-1}$  that have been assigned tentatively to protonation and/or conformational changes of subunit I residues Glu242 and Asp51, respectively.<sup>25–27</sup> Other features of reduced minus oxidized IR spectra of bovine and other forms of CcO have been discussed extensively elsewhere.<sup>20,28–31</sup>

Formate binding was initiated by perfusion of “fast” oxidized CcO with 10 mM formate for 3 min. After this treatment, free formate was removed by switching to formate-free buffer without measurable loss of the formate-induced difference spectrum. The features at 412, 434, 536, 583, and 640 nm (Figure 1D) are consistent with reported formate-ligated minus unligated fast oxidized difference spectra,<sup>6</sup> and their persistence in the absence of formate is consistent with the lack of reversibility of binding.<sup>21</sup> Quantitation relative to the redox spectrum of Figure 1C using extinction coefficients of  $\Delta\epsilon_{414-430} = 34.5 \text{ mM}^{-1}$  (formate minus unligated) and  $\Delta\epsilon_{446-416} = 209.6 \text{ mM}^{-1}$  (reduced minus oxidized)<sup>24</sup> indicated a yield of 90% of the formate-ligated form.

The corresponding formate-ligated minus unligated ATR-FTIR difference spectra (after exchange to formate-free perfusant) are shown in Figure 2, traces C (<sup>12</sup>C formate in H<sub>2</sub>O), D (<sup>12</sup>C formate in D<sub>2</sub>O), and E (<sup>13</sup>C formate in H<sub>2</sub>O). For comparison, the lower panel of Figure 2 shows the absolute IR spectra of <sup>12</sup>C formate in H<sub>2</sub>O (trace F), <sup>12</sup>C formate in D<sub>2</sub>O (trace G), <sup>13</sup>C formate in H<sub>2</sub>O (trace H), and <sup>12</sup>C formic acid in H<sub>2</sub>O (trace I). The bands at 1581 and 1353  $\text{cm}^{-1}$  in the formate spectrum (Figure 2F) have been assigned to the antisymmetric and symmetric carboxylate (COO<sup>-</sup>) stretching modes, and the 1384  $\text{cm}^{-1}$  band has been assigned to CH deformation.<sup>32</sup> In formic acid itself (trace I), these bands are replaced by ones at 1719 and 1214  $\text{cm}^{-1}$  that can be assigned to the  $\nu(\text{C}=\text{O})$  and  $\nu(\text{C}-\text{O})$  carboxylic bands.<sup>33</sup> H/D exchange (Figure 2G) causes a 10  $\text{cm}^{-1}$  upshift of the antisymmetric COO<sup>-</sup> stretching band, but has little effect on the symmetric COO<sup>-</sup> stretching or CH deformation bands. <sup>13</sup>C substitution (Figure 2H) causes a 40  $\text{cm}^{-1}$  downshift of the antisymmetric COO<sup>-</sup> stretching band and a 23  $\text{cm}^{-1}$  downshift of the CH deformation band.

After binding of formate to CcO in H<sub>2</sub>O media, prominent peaks were observed at 1576, 1376, and 1346  $\text{cm}^{-1}$  (Figure 2C). They were little affected by H/D exchange (Figure 2D) but shifted to 1533, 1374, and 1337  $\text{cm}^{-1}$  when <sup>13</sup>C-labeled formate was used as ligand (Figure 2E). Hence, the 1576 and 1346  $\text{cm}^{-1}$  bands can be assigned to the antisymmetric and symmetric COO<sup>-</sup> stretching, and the 1376  $\text{cm}^{-1}$  band can be assigned to CH deformation modes of ligated formate. The 230  $\text{cm}^{-1}$  frequency difference between the antisymmetric and symmetric COO<sup>-</sup> bands of formate indicates that both oxygen atoms of formate are ligated, either as a bidentate ligand to heme

*a*<sub>3</sub> or with one oxygen ligated to heme *a*<sub>3</sub> and the other to Cu<sub>B</sub>.<sup>34</sup> The narrowing of the 1576/1533  $\text{cm}^{-1}$  peak in comparison to the equivalent band of the free form indicates steric and environment constraints within the binding site, and H/D insensitivity of 1576  $\text{cm}^{-1}$  suggests that the bound formate is beyond the influence of bulk water. The lack of any positive band in the 1720–1710  $\text{cm}^{-1}$  region that would correspond to the carboxylic stretch of protonated formic acid (Figure 2I) demonstrates unequivocally that the ligand is bound as an anion. If it is assumed that the extinction coefficients of formate remain the same in bound and free forms, the amount of bound formate can be estimated to be equivalent to 560  $\mu\text{M}$  in solution by comparison of the areas of the COO<sup>-</sup> mode at 1576 (<sup>12</sup>C form)/1533 (<sup>13</sup>C form)  $\text{cm}^{-1}$  measured in CcO and model compounds. If the CcO (rough monomer dimensions of 100 Å diameter × 120 Å height<sup>1</sup>) were packed to a maximum density with no solvent spaces, the concentration of CcO would be around 1.76 mM. Since the extent of formate ligation was roughly 90% by quantification from visible spectra (Figure 1) and with the assumption that each CcO has a single formate binding site, it may be deduced that CcO in the rewetted state occupies roughly one-third of the IR-accessible volume of the protein film. These relative values seem reasonable given that protein packing is imperfect, with inevitable spaces that will be occupied by solvent and lipid. Future comparisons with comparable ratios for other bound ligands will provide a novel means of determination of ligand/protein relative stoichiometries.

Other features can be assigned to perturbations of ferric heme *a*<sub>3</sub> and surrounding protein that are induced by formate binding. Although the 1690–1620  $\text{cm}^{-1}$  region is often dominated by amide I changes, the peaks/troughs at 1692/1677, 1662/1651, and 1612  $\text{cm}^{-1}$  can be assigned tentatively to changes primarily in the vibrational modes of the propionic,<sup>35</sup> formyl, and vinyl<sup>28,36–38</sup> substituents of heme *a*<sub>3</sub>. Changes in the 1560–1520  $\text{cm}^{-1}$  region are generally dominated by amide II<sup>39</sup> and heme ring bands.<sup>40</sup> The trough/peak at 1233/1216  $\text{cm}^{-1}$  is also in a region where heme ring changes are expected.<sup>40</sup>

When experiments were performed in D<sub>2</sub>O media, difference spectra (Figure 2D) were dominated by a trough at 1549  $\text{cm}^{-1}$  and an accompanying peak at 1448  $\text{cm}^{-1}$ . Such a shift is indicative of a shift of the amide II band caused by additional H/D exchange. This irreversible band shift occurred regardless of the length of preincubation in D<sub>2</sub>O media and suggests that the weak anion formate might act as a catalyst for H/D exchange of parts of the protein structure that are otherwise resistant to H/D exchange. However, the extent of changes was less than 1% of total amide II and did not obscure the underlying changes caused by ligand binding at the binuclear center.

A point that is likely to be relevant to the chemistry involved in the proton/electron coupling mechanism is the nature of the protonation site that changes when the formate binds in order

- (26) Hellwig, P.; Soulimane, T.; Buse, G.; Mäntele, W. *FEBS Lett.* **1999**, *458*, 83–86.  
 (27) Okuno, D.; Iwase, T.; Shinzawa-Itoh, K.; Yoshikawa, S.; Kitagawa, T. *J. Am. Chem. Soc.* **2003**, *125*, 7209–7218.  
 (28) Hellwig, P.; Grzybek, S.; Behr, J.; Michel, H.; Mäntele, W. *Biochemistry* **1999**, *38*, 1685–1694.  
 (29) Hellwig, P.; Behr, J.; Ostermeier, C.; Richter, O.-M. H.; Pfizner, U.; Odenwald, A.; Ludwig, B.; Michel, H.; Mäntele, W. *Biochemistry* **1998**, *37*, 7390–7399.  
 (30) Lübken, M.; Prutsch, A.; Mamat, B.; Gerwert, K. *Biochemistry* **1999**, *38*, 2048–2056.  
 (31) Nyquist, R. M.; Heitbrink, D.; Bolwien, C.; Wells, T. A.; Gennis, R.; Heberle, J. *FEBS Lett.* **2001**, *505*, 63–67.  
 (32) McGrath, R.; Ledieu, J.; Cox, E. J.; Haq, S.; Diehl, R. D.; Jenks, C. J.; Fisher, I.; Ross, A. R.; Lograsso, T. A. *J. Alloys Compd.* **2002**, *342*, 432–436.  
 (33) Barth, A. *Prog. Biophys. Mol. Biol.* **2000**, *74*, 141–173.

- (34) Gibson, D. H.; Ding, Y.; Miller, R. L.; Sleadd, B. A.; Mashuta, M. S.; Richardson, J. F. *Polyhedron* **1999**, *18*, 1189–1200.  
 (35) Behr, J.; Hellwig, P.; Mäntele, W.; Michel, H. *Biochemistry* **1998**, *37*, 7400–7406.  
 (36) Callahan, P. M.; Babcock, G. T. *Biochemistry* **1983**, *22*, 452–461.  
 (37) Ching, Y.-C.; Argade, P. V.; Rousseau, D. L. *Biochemistry* **1985**, *24*, 4938–4946.  
 (38) Han, S.; Ching, Y.; Hammes, S. L.; Rousseau, D. L. *Biophys. J.* **1991**, *60*, 45–52.  
 (39) Mäntele, W. In *Biophysical Techniques in Photosynthesis*; Ames, J., Hoff, A. J., Eds.; Kluwer Academic Publishers: Dordrecht, 1996; pp 137–160.  
 (40) Berthomieu, C.; Boussac, A.; Mäntele, W.; Breton, J.; Nabdryk, E. *Biochemistry* **1992**, *31*, 11460–11471.

to maintain electroneutrality. The IR data show definitively that the bound ligand is in its anionic form. Hence, the charge-compensating protonation change that is linked to formate binding<sup>19</sup> must arise from a change elsewhere in the structure. Scrutiny of the structure indicates that glutamic acid (E242), tyrosine (Y244), or histidine (H290, H291, H376) residues that are directly involved in the binuclear site are possible alternative candidates. Changes in the 1760–1710  $\text{cm}^{-1}$  region can in general be attributed to carboxylic groups. In bovine CcO a heterogeneous peak/trough at 1749/1741  $\text{cm}^{-1}$  appears in CO photolysis spectra,<sup>27,41,42</sup> a more complex pattern is found in cyanide photolysis spectra,<sup>42</sup> and a pair of troughs occurs at 1748 and 1737–6  $\text{cm}^{-1}$  in reduced minus oxidized difference spectra<sup>25–27</sup> that are H/D sensitive (Figure 2A). The band changes above 1740  $\text{cm}^{-1}$  have been associated with perturbation or deprotonation of Glu242 in response to CO photolysis or heme *a* redox change. The peak/trough at 1748/1741  $\text{cm}^{-1}$  in the formate binding spectrum that also appears to be H/D sensitive (Figure 2C,D) most likely also arises from some perturbation of this residue. However, the lack of a major net positive feature in this region rules out significant protonation of a carboxylate group. Similarly, the binding spectra argue against heme propionate protonation from the lack of a positive band around 1700  $\text{cm}^{-1}$ <sup>35</sup> and tyrosinate protonation from the lack of any prominent peak/trough around 1518/1498  $\text{cm}^{-1}$ .<sup>33,43</sup> However, changes of protonation state of metal-ligated histidine are expected to occur in the 1075–1130  $\text{cm}^{-1}$  region<sup>44,45</sup> and peak/troughs at 1117/1105 and 1100/1088  $\text{cm}^{-1}$  are indeed present in the formate-binding spectra (Figure 2C–E). The histidine ligand to  $\text{Cu}_B$ , His240, cannot be a protonation site since its N1 ( $\text{N}\tau$ ) and N3 ( $\text{N}\pi$ ) nitrogens are linked respectively to Tyr244 and  $\text{Cu}_B$ .<sup>1</sup> However, it is possible that three other histidine ligands that ligate through their N1 nitrogens to the iron of heme *a*<sub>3</sub> (His376) or to  $\text{Cu}_B$  (His290 and His291), might provide a protonation site at their free N3 positions. Indeed, one of these histidine ligands to  $\text{Cu}_B$  was initially thought to provide a protonation site when adopting an orientation such that it became dissociated from  $\text{Cu}_B$ ,<sup>2</sup> although such an orientation is now thought unlikely<sup>46</sup> and electrostatic calculations indicate that all of these histidines are likely to be in the

neutral form with the N3 position already protonated.<sup>47,48</sup> Metal-bound histidine in its neutral (protonated) form is expected to have a C5N1 band in the 1103–1112  $\text{cm}^{-1}$  region that is insensitive to H/D exchange.<sup>44</sup> Hence, it is feasible that the H/D-insensitive 1117/1105  $\text{cm}^{-1}$  peak/trough arises from perturbation of neutral histidine ligands. A second H/D-insensitive trough at 1088  $\text{cm}^{-1}$  in the formate-binding spectra could, however, arise from an anionic histidine that is bound to a metal via its N1 nitrogen,<sup>49</sup> becoming protonated and moving to higher frequency when formate binds. This therefore leaves candidates for charge compensation of an anionic histidine metal ligand or, more likely, a hydroxide ligand to heme *a*<sub>3</sub> or  $\text{Cu}_B$ , both of which are likely to be hydroxide-ligated in the “fast” oxidized form of CcO,<sup>8,9</sup> and one of which is displaced on binding of the anionic formate to maintain a net electroneutral charge change within the binuclear center.

## Conclusion

Perfusion ATR-FTIR spectroscopy has demonstrated that the IR signature of binding of ligands such as formate to the heme *a*<sub>3</sub>– $\text{Cu}_B$  binuclear site of CcO is feasible and quantifiable. The data here show unequivocally that formate binds in its anionic form despite its binding being electroneutral overall. The bound formate can be distinguished from free ligand by the binding-induced sharpening and downshifting of vibrational bands. Formate ligation also causes shifts of vibrational modes of heme *a*<sub>3</sub> and its substituents and perturbation of histidine residues. The association of the accompanying protonation change with a carboxylate or tyrosine can be ruled out and may involve a histidine metal ligand or, more likely, a simple displacement into the bulk phase of a hydroxide ligand to heme *a*<sub>3</sub> or  $\text{Cu}_B$ , a reaction which would account for stoichiometric proton uptake and maintenance of net charge within the binuclear center domain.

**Acknowledgment.** This work was supported by The Wellcome Trust (Grant 062827). We thank Mr. Jonathan Ramsey and Mr. Santiago Garcia for expert technical support.

JA039320J

(41) Dyer, R. B.; Peterson, K. A.; Stoutland, P. O.; Woodruff, W. H. *Biochemistry* **1994**, *33*, 500–507.

(42) Rich, P. R.; Breton, J. *Biochemistry* **2001**, *40*, 6441–6449.

(43) Flemming, D.; Hellwig, P.; Friedrich, T. *J. Biol. Chem.* **2003**, *278*, 3055–3062.

(44) Hasegawa, K.; Ono, T.-A.; Noguchi, T. *J. Phys. Chem. A* **2002**, *106*, 3377–3390.

(45) Berthomieu, C.; Hienerwadel, R. *Biochemistry* **2001**, *40*, 4044–4052.

(46) Ostermeier, C.; Harrenga, A.; Ermler, U.; Michel, H. *Proc. Natl. Acad. Sci. U.S.A.* **1997**, *94*, 10547–10553.

(47) Yoshikawa, S.; Shinzawa-Itoh, K.; Nakashima, R.; Yaono, R.; Yamashita, E.; Inoue, N.; Yao, M.; Fei, M. J.; Libeu, C. P.; Mizushima, T.; Yamaguchi, H.; Tomizaki, T.; Tsukihara, T. *Science* **1998**, *280*, 1723–1729.

(48) Kannt, A.; Lancaster, R. D.; Michel, H. *Biophys. J.* **1998**, *74*, 708–721.

(49) Noguchi, T.; Inoue, Y.; Tang, X.-S. *Biochemistry* **1999**, *38*, 10187–10195.